

First Data on Vertical Particle Fluxes and Environmental Conditions in the Northern Segment of the Mohns Ridge, Norwegian Sea

A. A. Klyuvitkin^{a,*}, M. D. Kravchishina^a, A. N. Novigatsky^a, N. V. Politova^a,
A. V. Bulokhov^a, and Corresponding Member of the RAS S. K. Gulev^a

Received July 12, 2023; revised August 3, 2023; accepted August 4, 2023

Abstract—Continuous two-year studies of particle fluxes and associated environmental parameters in the axial zone of the Arctic segment of the Mid-Atlantic Ridge at the junction of the Mohns and Knipovich ridges (Norwegian Sea) have been carried out for the first time. Sediment traps were deployed from the R/V *Akademik Mstislav Keldysh* in June 2019 in the northeastern part of the Mohns Ridge with revision in August 2020 and lifting in July 2021. It is shown that the sedimentation of particles in the study area was affected by the global transport of water masses in the northeasterly direction, with Atlantic waters in the subsurface layer and water masses of Arctic origin recirculating deeper in the subsurface. A weak positive temperature trend at a depth of more than 2500 m (0.02°C over two years) is detected. The bimodal vertical distribution of fluxes and changes in the composition of sinking particles corresponded to the pattern of sediment recycling in the ocean. The annual course of fluxes in the subsurface layer is determined by the activity of Si-concentrating and calcifying plankton, while the maximum bloom period is also manifested in the deep layer. At the same time, the main significant source of the flux deeper than 2000 m is the supply of lithogenic matter from the near-bottom nepheloid layer.

Keywords: Arctic region, Arctic Ocean, sediment traps, lateral flux, currents, organic matter, biogenic silica, calcium carbonate, Atlantification

DOI: 10.1134/S1028334X23601840

INTRODUCTION

The dispersed sedimentary matter suspended in the kilometers-thick water column of the oceans is the material that ultimately forms bottom sediments and sedimentary rocks [1]. Particle fluxes in the ocean are one of the main characteristics of sedimentation, which allows for the dynamic study of sedimentation processes and transformation of sediments as they pass through the water column and makes it possible to estimate the quantity and determine the composition of particles settling to the ocean floor. These studies have been carried out in the World Ocean within the framework of the Leading Scientific School of Academician A.P. Lisitzin over the last half-century [1].

The Norwegian Sea serves as a transit zone through which the warm and salty Atlantic Water (AW) is transported from the North Atlantic to the Arctic Ocean [2, 3]. This zone is the main thermal reservoir of Subarctic seas and, at the same time, is an energetically active zone that directly affects the climate in

Europe and the further inflow of AW into the Barents Sea and Fram Strait [4].

A considerable number of studies deals with the processes of sedimentation and the mechanisms of its formation in this region [5–8], most of which, however, were conducted in the 1980s–1990s [6–8]. At the same time, in the early 2000s, the stage of Arctic Ocean “Atlantification” began, leading to intensified heat transport through the Norwegian Sea in the northerly and northeasterly directions [9, 10]. The Norwegian Sea has a tendency toward an increase in the water temperature in both the surface and deeper layers, due to the increased heat content of AW. To assess the potential impact of climate changes on the quantitative characteristics of sedimentation processes in this area, the data on particle fluxes and composition, as well as the scale of seasonal variability, need updating. Among the reasons for choosing a particular point for our efforts was the desire to study the possible influence of inflow of hydrothermal particles with a neutrally buoyant plume in the axial zone of the Arctic segment of the Mid-Atlantic Ridge near the junction area of the Mohns and Knipovich ridges.

Thus, the aim of our study was to investigate the vertical particle fluxes in the Norwegian Sea (Fig. 1) based on data collected over two years by the

^a Shirshov Institute of Oceanology, Russian Academy of Sciences, Moscow, Russia

*e-mail: klyuvitkin@ocean.ru

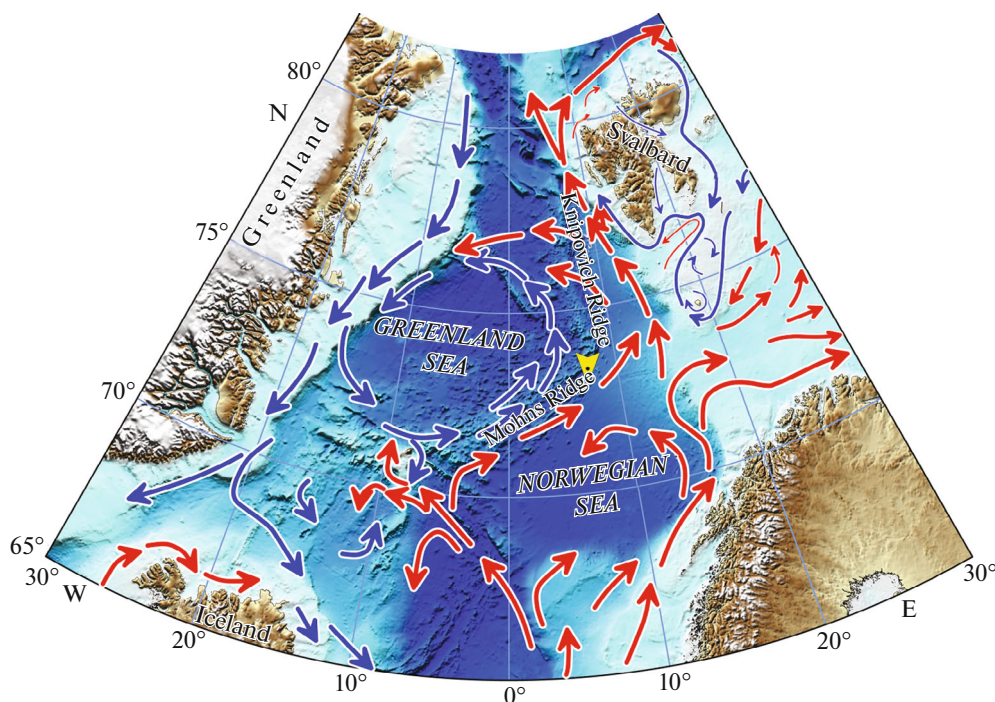


Fig. 1. Schematic map of the Norwegian–Greenland Basin: blue arrows mark the directions of movement for polar water; red arrows designate the directions of movement for Atlantic Ocean water according to [12, 13]. The yellow triangle shows the ADOS site.

Automatic Deep-Water Sedimentary Observatory (ADOS [11]).

MATERIALS AND METHODS

The material for our study was collected for over two years (779 days) from June 2019 (the 75th cruise of the R/V *Akademik Mstislav Keldysh* [14]) until July 2021 (the 84th cruise of the R/V *Akademik Mstislav Keldysh* [15]) with the revision and reloading of the observatory in August 2020 (the 80th cruise of the R/V *Akademik Mstislav Keldysh* [16]) in the northern segment of the Mohns Ridge. Sinking particles was collected in differential 12-bottle conical Lotos-3 sediment traps with a sampling area of 0.5 m², produced by the Experimental Design Bureau of Oceanological Engineering, Russian Academy of Sciences (the sampler replacement interval was 30 days), and in integrated small cylindrical MSL-110 sediment traps with a sampling area of 0.0095 m², manufactured by the Shirshov Institute of Oceanology, Russian Academy of Sciences [17]. The ADOS scheme is shown in Fig. 2. Lotos-3 traps were deployed below the upper active layer (500 m) and 330 m above the seafloor to minimize the influence of the near-bottom nepheloid layer and were additionally equipped with integrated traps. MSL-110 traps were placed in the intermediate layers (between the conical ones). In total, samples were collected from six layers. To prevent biological transformation of the collected matter, the sampling bottles were filled with HgCl₂ solution (1% saturated solu-

tion) based on the filtrate of seawater from the sampling area. NaCl was added to the solution to make its salinity equal to 45 psu.

Nortek Aquadopp acoustic current meters were set in the deployment layers of 12-bottle traps, and the deployment layers of MSL-110 were additionally equipped with RBRduet temperature and pressure sensors to determine the source of sediment transport and to estimate the lateral component of the matter flux at ADOS.

When deployment, revising, and lifting the traps using the SBE911 onboard profiling system equipped with Niskin bottles, seawater samples were taken to study the characteristics of the water column, including suspended matter. The sedimentary matter collected in the traps and suspended particulate matter were then processed according to a uniform procedure for all samples [5, 11, 18]. The contents of Si and Al were determined by a photometric method modified by A.B. Isaeva for suspended matter (accuracy of 2–5%). C_{total} and C_{carb} were estimated using a TOC-L Shimadzu analyzer with an SSM-5000A tool; C_{org} was calculated by the difference in the C_{total} and C_{carb} contents in the sample. The measurement error was 1%; the reproducibility of the analysis results was $\pm 5\%$. The content of organic matter (OM) was determined as doubled C_{total} , based on the conventional research practice [8, 11, 18]. CaCO₃ was calculated stoichiometrically from C_{carb} , and the lithogenic material (LM) was determined from Al, by multiplying by 12.27,

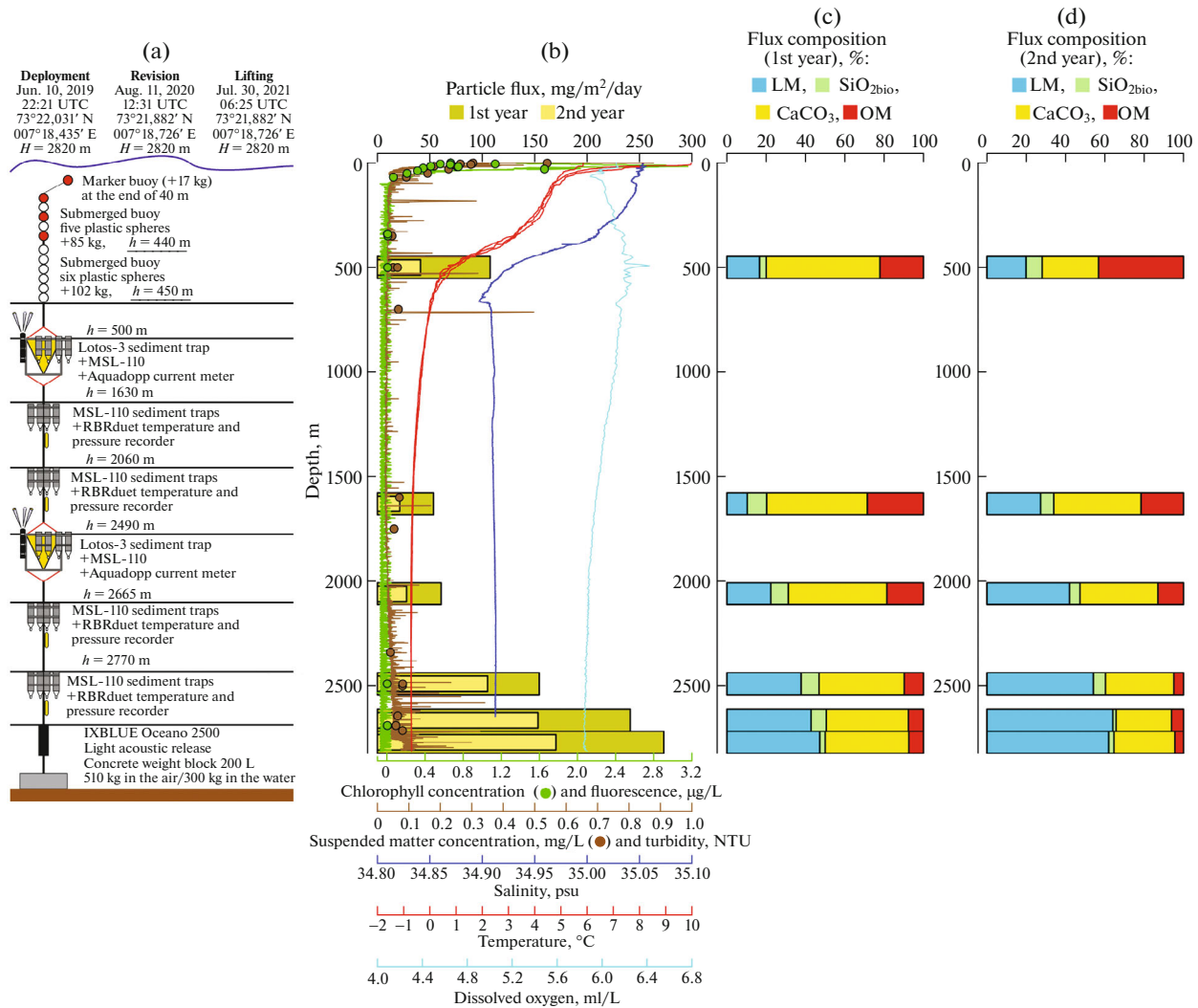


Fig. 2. (a) Diagram of ADOS; (b) vertical distribution of annual total vertical particle fluxes and water column parameters during the deployment, revision, and lifting of ADOS; composition of settling material during the (c) 1st and (d) 2nd years of ADOS operation.

while biogenic silica (SiO_{2bio}) was obtained using the terrigenous matrix method based on the difference between the total and lithogenic SiO₂ contents, using the average composition of the upper layer of the Earth's crust [19]. The sum of LM, OM, CaCO₃, and SiO_{2bio} averaged 100% with a slight deviation within 15%.

To calculate the average concentrations of chlorophyll-a (Chl-a) in the surface layer of the sea in the research area, we used the data derived from the MODIS-Aqua satellite ocean color scanner (<https://oceancolor.gsfc.nasa.gov/>).

RESULTS

Water column. CTD profiling of the water column during the deployment, revision, and lifting of ADOS showed (Fig. 2) that the upper 400 m of the water col-

umn (excluding the seasonally heated quasi-homogeneous surface layer less than 20 m thick) is occupied by AW, which is relatively warm (3–5°C) and saline (35.0–35.05 psu). No pronounced interannual temperature fluctuations were observed in the AW layer. Deeper, there are Arctic intermediate waters of the Norwegian Sea (temperature from –0.5 to 0.5°C, salinity of 34.9 psu), characterized by a weakly enhanced dissolved oxygen content in the 500–700 m layer [12]. Lower to the bottom is the Norwegian Sea Deep Water with a characteristic temperature below –0.7°C and salinity of 34.91 psu.

The concentrations of suspended particulate matter in the water column varied from relatively high values of 0.18–0.54 mg/L in the upper productive layer (0–50 m) to minimum values of 0.04–0.08 mg/L in the deep layers. In this case, the surface waters (0–25 m) were characterized by relatively high concentrations of

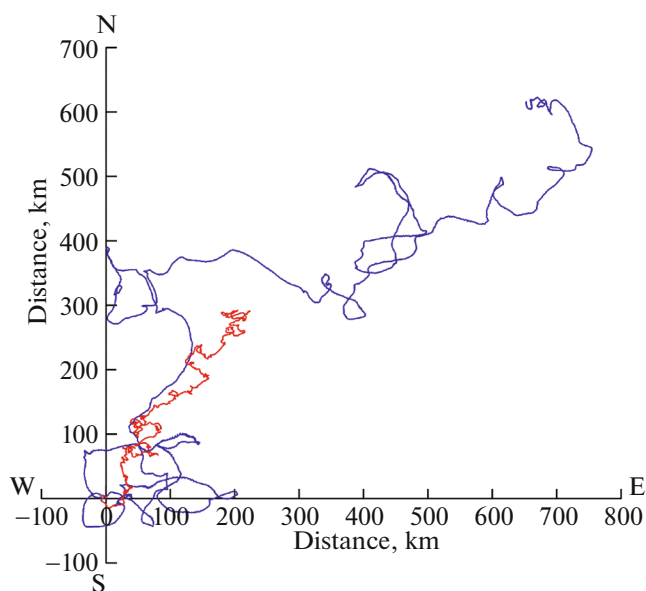


Fig. 3. Progressive vector diagram of currents in the subsurface depth of 500 m (blue line) and in the deepwater depth of 2490 m (red line).

Chl-a ($0.46\text{--}1.65\ \mu\text{g/L}$). The vertical distribution of Chl-a showed the presence of a subsurface maximum (15–35 m). As the depth increased to 50 m, the Chl-a concentrations gradually decreased to $0.1\text{--}0.2\ \mu\text{g/L}$, and below 100 m they were the lowest ($\leq 0.01\ \mu\text{g/L}$). No significant interannual variation was observed in the distribution of suspended matter and Chl-a over two years of observation. The maximum Chl-a was recorded in June 2019 and corresponds to the beginning of the spring bloom of phytoplankton.

Currents. The transport of water masses throughout the entire water column occurred in the northeasterly direction (Fig. 3). In the years 2019–2020, the flow was directed in general to the north-northeast, while in the years 2020–2021 it turned to the east-northeast. The near-bottom layer did not undergo such changes. The total accumulated displacement of water masses in the subsurface layer was 897 km, while in the deep layer it was 367 km. The current velocity in the subsurface layer varied from 0 to 32.3 cm/s at an average value of 7.3 cm/s. In the deep layer, the current velocities did not exceed 13.7 cm/s at an average value of 2.7 cm/s. The current velocity was recorded to increase almost synchronously in both layers in March–April of 2020 and 2021, with prevailing northerly currents. Similar seasonal spikes in the current velocity were also observed in the subsurface layer in December 2019 and 2020.

Temperature. Two-year temperature measurements showed a synchronous weak increase in temperature of about 0.02°C in the depth of the overbottom (2665 m) and near-bottom (2770 m) MSL-110 traps (Fig. 4f). Above, in the layers of 500 and 2490 m, there were no similar trends; however, temperature sensors

with low resolution of 0.01°C were mounted into the current meters in these layers.

Total particle fluxes. The vertical distribution of annual total fluxes of matter is characterized by bimodality (Fig. 2): maximum in the subsurface layer, minimum in the intermediate waters in the dissolution layer [1], and a sharp increase in the flux magnitude in the benthic nepheloid layer. An increase in turbidity in the near-bottom layer was recorded by a LISST-Deep laser particle analyzer and a nephelometer as part of the onboard profiling system during the deployment, revision, and lifting of ADOS. Based on the profiling data, the nepheloid layer extended from the seafloor (2820 m) to ~ 2000 m, and thus, its thickness exceeded 800 m. An almost twofold decrease in flux magnitudes was established during the second ADOS exposure; however, the total bimodal distribution repeats in both observation periods.

The processing of the materials collected in the differential traps revealed a pronounced annual course of particle fluxes in the subsurface (500 m) layer. The largest fluxes occur during the summer months (June–September) with an absolute maximum in July 2019, $274\ \text{mg/m}^2/\text{day}$. A similar annual course of Chl-a distribution in the surface layer was also revealed by the analysis of data derived from the Aqua-MODIS satellite ocean color scanner (Fig. 4a). From November to May, fluxes are smallest at a depth of 500 m. In the deep layer, the first period of ADOS operation is characterized by a bimodal pattern for distribution of fluxes in time with maxima in June–July 2019 and April–May 2020, when fluxes sharply increased to $256\ \text{mg/m}^2/\text{day}$, almost reaching the summer maximum of the previous year. The second year of ADOS operation in the deep layer was characterized by the smoother annual course of flux magnitudes, among which a local minimum of fluxes was observed in November–December 2020.

No pronounced interannual variation was detected in the flux magnitudes. Only a significant decrease in fluxes from the surface ocean layer was observed in June–July 2021 compared to the same period in 2019. Data on fluxes for June–July 2020 are absent.

The annual course of fluxes corresponds to the changes in the sound backscatter coefficient by suspended matter according to the data of the acoustic current meters operating at the same layers (Figs. 4b, 4c). In June–July 2020, these data show an increase in acoustic scattering, which may indicate a significant increase in particle fluxes. However, unfortunately, this period remained uncovered for collection of matter in the differential traps since the revision and rearrangement of the ADOS in 2020 became possible only two months after the annual cycle of sedimentary matter collection in the traps of the first term of observations had been completed.

The composition of sedimentary matter. The upper layers (500 m and 1630 m) matter consist mainly of

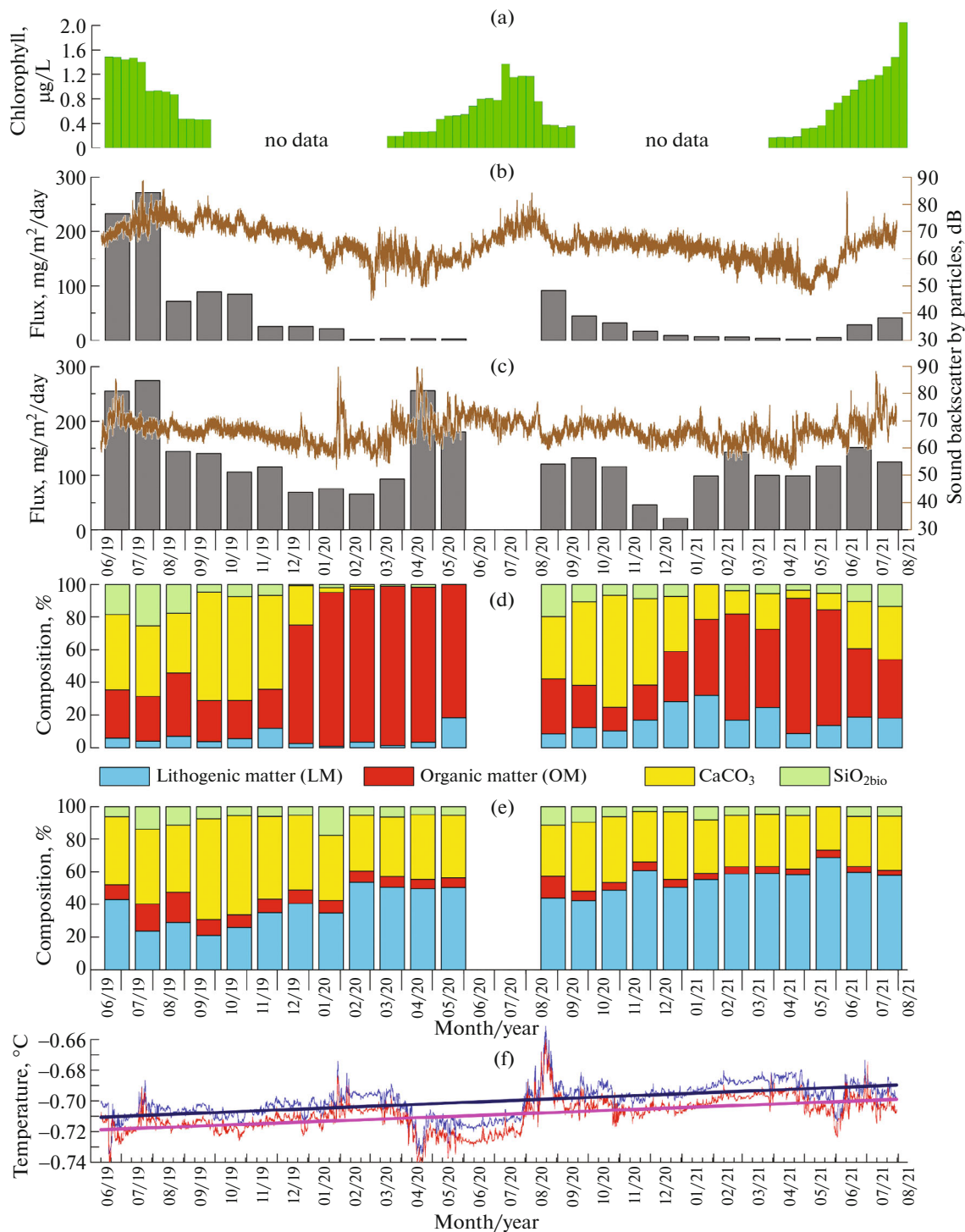


Fig. 4. (a) Chlorophyll-a content in the ocean surface layer according to the satellite data; vertical particle fluxes of sedimentary material and sound backscatter by sedimentary particles (b) in the subsurface layer at 500 m and (c) in the deepwater layer at 2490 m; composition of the settling matter (d) in the subsurface layer at 500 m and (e) in the deepwater layer at 2490 m; (f) temperature at 2665 m (red line) and 2770 m (blue line) and corresponding trend lines.

biogenic material (BM) with a large number of planktonic organisms (zooplankton, ostracods, etc.). In the deep layers from 2060 m to the ocean floor, there is only a dense brown sediment almost without heterogeneous biogenic remains; lithogenic material (LM) is

observed in the MSL-110 samplers. This is confirmed by the study data of the main components of the settling matter. The surface and intermediate layers are dominated by BM (as the sum of OM, CaCO_3 , and $\text{SiO}_{2\text{bio}}$), 89%, while the proportion of LM increases

starting from 2000 m and reaches its maximum in the near-bottom layer, 60–64%.

A pronounced annual variation in the composition of biogenic material in the subsurface layer is recorded. CaCO_3 dominated (37–69%), OM ranged from 14 to 39%, and the proportion of $\text{SiO}_{2\text{bio}}$ was 7–25% from June to December of 2019 and 2020. The peak of $\text{SiO}_{2\text{bio}}$ (18–25%) occurred in June–August. In the winter months (December–May), when the total flux values are the smallest, the LM content increases by a factor of three (up to 33%).

In the deep-water layer, the annual fluctuations in the flux composition were insignificant and corresponded to the average composition according to the data of annual MSL-110 traps. There is a slight decrease in the LM proportion from July to October, being more pronounced in 2019.

DISCUSSION

Based on the cumulative vector transport of water masses through the observation point and the average concentrations of suspended matter over three years of studies, the lateral particle flux is calculated as 69.0 and 37.6 $\text{g/m}^2/\text{day}$ in the subsurface and deep-water layers, respectively. These values are three orders of magnitude higher than the vertical particle flux determined using the sediment traps. This suggests that only about 0.1–0.4% of the particles are settling near the source; all the rest are transported laterally, primarily to the northeast. In the deep-water layer, the proportion of settling particles is higher (0.4%) due to the lower current velocities. However, this is much greater than, for example, on the eastern slope of the Lofoten Basin in the Norwegian Sea [20].

The increasing hydrodynamic activity of the environment in March–April was reflected in the short-term deepening of the tools due to the inclination of the ADOS by the flow. The maximum deepening of the tools was recorded in March, and in the subsurface layer it reached about 50 m, while in the deep layer it was 8 m relative to the specified layer of the tool operation. These values are significantly lower than those we observed in 2018–2019 in the Lofoten Basin (270 and 19 m, respectively). Thus, the ADOS working area is characterized by a quieter hydrodynamic regime of water compared to the nearby Lofoten Basin, and the particles that move from the south and southwest of the Norwegian Sea and do not settle due to high current velocities can be deposited here. Therefore, the mass fluxes of particles in the subsurface layer obtained in this study might be higher than in the Lofoten Basin [5]. In the near-bottom layer, the fluxes in the Lofoten Basin are higher evidently due to more intense turbidity and redeposition of particles in the nepheloid layer at higher current velocities.

The annual total fluxes decreased significantly in the second year of ADOS operation due to the collec-

tion of material in the MSL-110 traps only during one period of the particle deposition maximum (June–July 2021), while the MSL-110 traps during the first year of operation covered the maximum values for 2019 and 2020. The maximum value in 2021 was not as significant as in the previous years, which is also confirmed by the distribution of sound backscatter by suspended matter according to the data of acoustic current meters and satellite-derived Chl-a data (Fig. 4). In general, the bimodal vertical distribution of fluxes and changes in their composition (the reduction in the BM proportion and the increase in the LM content as the distance to the bottom decreases) correspond to the recycling scheme of settling matter in the ocean [1].

The results of analyzing the satellite data of Chl-a distribution together with the values of total fluxes of particles and variability in composition of settling particles showed that the annual course of fluxes in the subsurface layer is determined by the activity of phytoplankton. Moreover, an increase in the proportion of $\text{SiO}_{2\text{bio}}$ during the months with spikes of both the total fluxes and Chl-a concentrations on the ocean surface (June–August) indicates an increased content of diatoms in the flux of detrital aggregates, being the main Si-concentrating phytoplankton in the study region [6, 8]. At the same time, the high content of CaCO_3 in the spring–summer months and its increase in the composition of the flux after the decline of diatom bloom in September–November indicates an increasing role of calcifying plankton, including pteropods, in the formation of the flux [5, 6, 8]. The local increase in total fluxes in September–October 2019 together with the increase in the CaCO_3 content is an example of this fact.

High fluxes in the subsurface layer in June–July 2019 are reflected in the deep layer in the same period, which manifests itself in the increase in both the mass flux and its biogenic component. At all other times, the peaks of fluxes in the subsurface and deep layers do not coincide. For example, a sharp increase in the flux at a depth of 2490 m in April–May 2019 was not manifested at a depth of 500 m at all. At the same time, according to the visual assessments, the volume of sedimentary matter collected in April did not increase as much, i.e., the sedimentary matter in April is characterized by a higher density compared to July and therefore differs in composition and origin. It is evident that the peak in July was caused by the influx of matter from the subsurface layer as a result of the seasonal increase in primary production, while the peak in April is related to the changes in the hydrological conditions and, consequently, to the increase in the hydrodynamic activity of the benthic nepheloid layer.

The bulk composition of particulate matter in the fluxes does not allow us to assess the possible contribution of particles of hydrothermal genesis that are delivered as a result of the distant transport of a neutrally buoyant plume from an undiscovered source. To

identify individual hydrothermal particles in the heterogeneous vertical flux, further precise research is required.

CONCLUSIONS

Continuous two-year research into particle fluxes and related environmental parameters in the axial zone of the Arctic segment of the Mid-Atlantic Ridge at the junction of the Mohns and Knipovich ridges was conducted for the first time.

It was shown that particle deposition in the study area was affected by global transport of the water masses in the northeasterly direction, with Atlantic waters being in the subsurface layer and Arctic water masses recirculating deeper. A weak two-year positive temperature trend was observed at depths greater than 2500 m.

The bimodal vertical distribution of the flux rates and the changes in the composition of settling particles corresponded to the recirculation scheme of settling particles in the ocean. The annual course of fluxes in the subsurface layer was determined by the activity of Si-concentrating and calcifying groups of plankton, with the peak bloom period being also in the deep layer. In this respect, the main significant source of flux below 2000 m is the input of lithogenic material from the benthic nepheloid layer.

ACKNOWLEDGMENTS

We are grateful to the crew members of the R/V *Akademik Mstislav Keldysh* and the researchers on board for their assistance in the field research.

FUNDING

This work was supported by the Russian Science Foundation, grant no. 20-17-00157 (<https://rscf.ru/project/20-17-00157/>). The data from the profilers were processed within the framework of the Notable Innovative Project of State Importance (NIPSI), agreement no. 169-15-2023-002. The field research was carried out in part under a State Assignment, subject no. FMWE-2021-0016.

CONFLICT OF INTEREST

The authors declare that they have no conflicts of interest.

OPEN ACCESS

This article is licensed under a Creative Commons Attribution 4.0 International License, which permits use, sharing, adaptation, distribution and reproduction in any medium or format, as long as you give appropriate credit to the original author(s) and the source, provide a link to the Creative Commons license, and indicate if changes were made. The images or other third party material in this article are included in the

article's Creative Commons license, unless indicated otherwise in a credit line to the material. If material is not included in the article's Creative Commons license and your intended use is not permitted by statutory regulation or exceeds the permitted use, you will need to obtain permission directly from the copyright holder. To view a copy of this license, visit <http://creativecommons.org/licenses/by/4.0/>.

REFERENCES

1. A. P. Lisitzin, in *The World's Ocean* (Nauchn. mir, Moscow, 2014), Vol. 2, pp. 331–571 [in Russian].
2. T. Rossby, M. D. Prater, and H. Søliland, *J. Geophys. Res.* **114**, C04011 (2009).
3. O. H. Segtnan, T. Furevik, and A. D. Jenkins, *J. Geophys. Res.: Oceans* **116**, C11003 (2011).
4. J. E. Ø. Nilsen and E. Falck, *Progr. Oceanogr.* **70** (1), 58–90 (2006).
5. A. V. Drits, A. A. Klyuvitkin, M. D. Kravchishina, V. A. Karmanov, and A. N. Novigatsky, *Oceanology* **60** (4), 501–518 (2020).
6. B. Bodungen, A. Antia, E. Bauerfeind, et al., *Geol. Rundsch.* **84**, 11–27 (1995).
7. S. Honjo, S. J. Manganini, R. A. Krishfield, and R. Francois, *Progr. Oceanogr.* **76**, 217–285 (2008).
8. R. Peinert, A. Antia, E. Bauerfeind, et al., in *The Northern North Atlantic: a Changing Environment*, Ed. by P. Schafer, W. Ritzrau, M. Schluter, and J. Thiede (Springer, Berlin, 2001), pp. 53–68.
9. S. Lind, R. B. Ingvaldsen, and T. Furevik, *Nat. Clim. Change* **8**, 634–639 (2018).
10. I. V. Polyakov, A. V. Pnyushkov, M. B. Alkire, et al., *Science* **365** (6335), 285–291 (2017).
11. A. P. Lisitsyn, V. N. Lukashin, A. N. Novigatskii, et al., *Dokl. Earth Sci.* **456** (2), 709–714 (2014).
12. J. Blindheim and S. Østerhus, *The Nordic Seas, Main Oceanographic Features* (Am. Geophys. Union, 2005), Vol. 158, pp. 11–37.
13. H. Loeng, *Polar Res.* **10** (1), 5–18 (1991).
14. A. A. Klyuvitkin, M. D. Kravchishina, I. A. Nemirovskaya, B. V. Baranov, A. I. Kochenkova, and A. P. Lisitzin, *Oceanology* **60** (3), 421–424 (2020).
15. M. D. Kravchishina, A. A. Klyuvitkin, V. D. Volodin, et al., *Oceanology* **62** (4), 572–575 (2022).
16. A. A. Klyuvitkin, N. V. Politova, A. N. Novigatsky, and M. D. Kravchishina, *Oceanology* **61** (1), 139–142 (2021).
17. V. N. Lukashin, A. A. Klyuvitkin, A. P. Lisitzin, and A. N. Novigatsky, *Oceanology* **51** (4), 699–704 (2011).
18. A. A. Klyuvitkin, A. N. Novigatsky, N. V. Politova, and E. V. Koltovskaya, *Oceanology* **59** (3), 411–422 (2019).
19. R. L. Rudnick and S. Gao, *Treatise Geochem.* **4**, 1–51 (2014).
20. V. N. Lukashin, *Sedimentary at the Continental Slopes under the Effect of Contour Flows* (GEOS, Moscow, 2008) [in Russian].

Translated by L. Mukhortova